Published online 23 October 2020 *Nucleic Acids Research, 2020, Vol. 48, No. 20* ***11615–11625***
doi: 10.1093/nar/gkaa903

Flexizyme-aminoacylated shortened tRNAs demonstrate that only the aminoacylated acceptor arms of the two tRNA substrates are required for cyclodipeptide synthase activity

Nicolas Canu[1], Carine Tellier[1], Morgan Babin[1], Robert Thai[2], Inès Ajel[1], Jérôme Seguin[1], Olivier Cinquin[1,3], Robin Vinck[2,3], Mireille Moutiez[1], Pascal Belin[1], Jean-Christophe Cintrat[3] and Muriel Gondry[1,*]

[1]Université Paris-Saclay, CEA, CNRS, Institute for Integrative Biology of the Cell (I2BC), 91198 Gif-sur-Yvette cedex, France, [2]Université Paris Saclay, CEA, INRAE, Département Médicaments et Technologies pour la Santé (DMTS), SIMoS, 91191, Gif-sur-Yvette, France and [3]Université Paris Saclay, CEA, INRAE, Département Médicaments et Technologies pour la Santé (DMTS), SCBM, 91191 Gif-sur-Yvette, France

Received June 17, 2020; Revised September 22, 2020; Editorial Decision September 28, 2020; Accepted September 30, 2020

ABSTRACT

Cyclodipeptide synthases (CDPSs) use two aminoacyl-tRNAs (AA-tRNAs) to catalyse cyclodipeptide formation in a ping-pong mechanism. Despite intense studies of these enzymes in past years, the tRNA regions of the two substrates required for CDPS activity are poorly documented, mainly because of two limitations. First, previously studied CDPSs use two identical AA-tRNAs to produce homocyclodipeptides, thus preventing the discriminative study of the binding of the two substrates. Second, the range of tRNA analogues that can be aminoacylated by aminoacyl-tRNA synthetases is limited. To overcome the limitations, we studied a new model CDPS that uses two different AA-tRNAs to produce an heterocyclodipeptide. We also developed a production pipeline for the production of purified shortened AA-tRNA analogues (AA-minitRNAs). This method combines the use of flexizymes to aminoacylate a diversity of minitRNAs and their subsequent purifications by anion-exchange chromatography. Finally, we were able to show that aminoacylated molecules mimicking the entire acceptor arms of tRNAs were as effective a substrate as entire AA-tRNAs, thereby demonstrating that the acceptor arms of the two substrates are the only parts of the tRNAs required for CDPS activity. The method developed in this study should greatly facilitate future investigations of the specificity of CDPSs and of other AA-tRNAs-utilizing enzymes.

INTRODUCTION

Cyclodipeptide synthases (CDPSs) constitute a family of tRNA-dependent enzymes involved in the biosynthesis of 2,5-diketopiperazines (2,5-DKPs) (1), a class of natural microbial products with therapeutically promising bioactivities, such as antibacterial, antifungal or antitumoral activity (2,3). CDPSs use two aminoacyl-tRNAs (AA-tRNAs), diverted from their canonical role in ribosomal protein synthesis, to catalyse the formation of various cyclodipeptides, the simplest members of the 2,5-DKP family (4).

CDPSs can be split phylogenetically into two subfamilies, named the NYH and XYP subfamilies according to the occurrence of two sets of conserved catalytic residues (5,6). Both subfamilies have been extensively studied (for reviews, see (1,7–9)). The catalytic mechanism used by AlbC from *Streptomyces noursei*, the first NYH CDPS to be identified, has been elucidated (10–12). It begins with the binding of the first substrate, Phe-tRNA^{Phe}, followed by the transfer and covalent attachment of its phenylalanyl moiety to a conserved serine residue, resulting in the formation of a phenylalanyl-enzyme intermediate. The second substrate, Leu-tRNA^{Leu}, interacts with the phenylalanyl-enzyme, to which its leucyl moiety is transferred, generating a dipeptidyl-enzyme intermediate. Finally, the dipep-

*To whom correspondence should be addressed. Tel: +33 169 08 76 47; Fax: +33 169 08 47 12; Email: muriel.gondry@i2bc.paris-saclay.fr
Present addresses:
Nicolas Canu, Toulouse Biotechnology Institute, 31300, Toulouse, France.
Jérôme Seguin, CEA, DEN, Centre de Marcoule, 30207 Bagnols-sur-Cèze, France.

tidyl moiety undergoes cyclization, with a conserved tyrosine residue acting as a proton relay, to yield the final cyclodipeptide cyclo(L-Phe-L-Leu) (cFL). The crystallographic structures of AlbC alone and in complex with a dipeptidyl intermediate analogue, and those of six other NYH or XYP CDPSs have been solved (10–11,13–15). Despite the very low levels of amino-acid sequence identity between CDPSs (below 10% in some cases), they share a common architecture, with a monomer built around a Rossmann fold domain that is very similar structurally to the catalytic domain of homodimeric class-Ic aminoacyl-tRNA synthetases (AARSs). The catalytic residues conserved throughout the CDPS family are located in the same position in all structures, strongly suggesting that all CDPSs, regardless of the subfamily to which they belong, act via similar mechanisms.

The two AA-tRNAs used successively as substrates by CDPSs are differently accommodated in the enzyme (11). The first substrate interacts with the enzyme through its aminoacyl moiety accommodated in a surface-accessible pocket named P1 and its tRNA moiety interacting either with basic residues at the surface of a conserved helix for NYH CDPSs (10,13–16) or basic residues present in the C- and N-terminal regions for XYP enzymes (17). The second substrate binds to the enzyme with its aminoacyl moiety accommodated in another pocket named P2 and the binding of its tRNA moiety is not documented (14,16). For each of the two substrates, the regions of the tRNA moieties essential for catalysis remains to be determined. In class-Ic AARSs, which have a conserved homodimeric quaternary structure, each monomer contains an anticodon-binding domain involved in recognizing the anticodon loop of a tRNA that is then acylated by the catalytic domain of the other monomer (18). CDPSs do not contain these anticodon-binding domains, almost all these enzymes are monomeric (1) and they use amino acids attached to the acceptor arm of tRNAs. They may not, therefore, be able to interact with the anticodon loop or another distal part of the tRNAs. Several studies had convergent results suggesting that the acceptors arms of the substrates were involved in the interaction with the enzyme (16,17). In order to further investigate the tRNA regions required for CDPS activity, an attractive strategy would involve the use of shortened tRNA analogues (minitRNAs), which have already proved valuable in the study of AARSs (19,20). Flexizymes, short AARS-like ribozymes, are a promising tool for the aminoacylation of diverse minitRNAs (21) but they have never been used for the study of AA-tRNA-utilizing enzymes. Flexizymes recognize their RNA acceptors by base-pairing with only three bases of their conserved 3′ termini. They can, therefore, accept a wide range of RNA acceptors as substrates: entire tRNAs, shortened tRNAs, such as microhelices (miHxs), and even tetramer oligonucleotides mimicking the 3′ NCCA tail of tRNA (21–23).

Here, we demonstrate using various flexizyme-aminoacylated minitRNAs (AA-minitRNAs) that the acceptor arms of the two substrates are the only parts of the tRNAs required for CDPS activity. To perform the study leading to this conclusion, we selected a new model CDPS that uses two different AA-tRNAs as substrates thus allowing to discriminate their bindings to the enzyme. We also produced relevant AA-minitRNAs thanks to the development of a new method combining the use of flexizymes with the separation of the AA-minitRNAs by anion-exchange chromatography. Finally, we set up an *in vitro* assay for the model CDPS, which allows to determine the behaviour of the CDPS towards its two AA-tRNA substrates and the produced AA-minitRNAs.

MATERIALS AND METHODS

Protein production

The His-tagged versions of T7 RNA polymerase, *Escherichia coli* AlaRS, *E. coli* GluRS and *Nbra*-CDPs were produced and purified according to published protocols ((24–26) and (4), respectively), modified slightly, as described in the detailed protocols in section I.A. of the Supplementary Data. The purified proteins were quantified by UV spectrophotometry with a DS-11 spectrophotometer (Denovix). Theoretical extinction coefficients were used for T7 RNA polymerase, *E. coli* AlaRS and *E. coli* GluRS. The experimental extinction coefficient of *Nbra*-CDPS was determined by acidic hydrolysis and amino-acid analysis (27).

Production of *Escherichia coli* tRNAs

Plasmids for the constitutive expression of $tRNA^{Ala}_{UGC}$, $tRNA^{Ala}_{GGC}$ and $tRNA^{Glu}$ (see Supplementary Table S1 for a summary of the sequences of all the RNAs used in this study) were constructed by inserting the corresponding tRNA sequences into pBSTNAV2, which was kindly provided by Pr. Yves Mechulam (section I.B.ii. of Supplementary Data and Supplementary Table S2). We generated the tRNAs according to a protocol provided by the team of Pr. Yves Mechulam, as detailed in (28) (see section I.B.ii of Supplementary Data). We quantified the tRNAs and all other RNAs used in this study by UV spectrophotometry with a DS-11 spectrophotometer (Denovix), assuming that 1 OD_{260nm} unit represented 40 ng/μl RNA.

Aminoacylation of tRNAs

The tRNAs were aminoacylated under the following conditions: 50 mM HEPES-KOH pH7.5, 20 mM KCl (only for $tRNA^{Ala}$), 15 mM $MgCl_2$, 1 mM or 10 mM dithiothreitol (DTT) for $tRNA^{Glu}$ and $tRNA^{Ala}$, respectively, 4 μM adenosine triphosphate (ATP), 15 μM tRNAs, 2 μM of the corresponding *E. coli* AARS and 250 μM of the corresponding L-amino acid. Reactions were incubated at 37°C for 20 min and stopped by adding sodium acetate pH 5.0 to a final concentration of 100 mM. The AA-tRNAs and the remaining non-acylated tRNAs were purified on a 5 ml Hi-Trap Q HP anion-exchange chromatography column (GE Healthcare), with a linear gradient of 0 to 1 M NaCl in 10 mM sodium acetate pH 5.0. Fractions containing tRNAs were subjected to ethanol precipitation and the precipitate obtained was stored as a dried pellet at −20°C. The proportion of aminoacylated tRNAs was determined by enzymatic assays, with high concentrations (500 nM) of *Nbra*-CDPS (section II.B.iii. of Supplementary Data).

Production of flexizymes (dFx) and minitRNAs

Microhelices (miHxs) mimicking the acceptor arms of *E. coli* tRNAs are abbreviated as miHx^{Yyy_X}. Yyy refers to the amino acid charged on the tRNA mimicked, and X is the number of base pairs retained in the stem (so, for example, miHx^{Ala_7} reproduces the entire acceptor arms of both tRNA^{Ala} isoacceptors, which are identical). MiHx^{Ala_4}, miHx^{Glu_7,} miHx^{Glu_3} and tetramer oligos ACCA and GCCA were synthesized chemically by Eurogentec. MiHx^{Ala_7} and dFx were synthesized by *in vitro* transcription and then purified by anion-exchange chromatography. *In vitro* transcription and treatment of the reactions were carried out using a protocol from the team of Prof. Suga (29), modified slightly to prevent the formation of template-independent transcripts (30) (see detailed protocol in section I.B.iv. of Supplementary Data). DNA matrices were obtained by mixing T7_F primer and the corresponding reverse primer (Supplementary Figure S1 and Table S3). After phenol extraction and removal of nucleotides and aborted transcripts using centrifugal filter, transcripts were renatured by heating at 80°C for 5 min and then rapidly decreasing the temperature to 4°C, before purification by HPLC on an Elite LaChrom HPLC system (VWR). Samples were loaded onto a DNAPAC-PA100 semi-preparative column (9 × 250 mm, 13.5 μm, Thermo Fisher Scienfitic). Separations were performed under non-denaturing conditions with an increasing linear gradient of buffer B (2.5 M ammonium acetate pH 5.2, 0.5% acetonitrile) in buffer A (25 mM ammonium acetate pH 5.2, 0.5% acetonitrile), at a flow rate of 5 ml/min (31). The gradient was optimized for each transcript, so a number of different gradients were used (Supplementary Table S4). Fractions of interest were desalted to 25 mM ammonium acetate pH 5.2 with a Hi-Trap 26-10 desalting column (GE Healthcare), freeze-dried and stored at −20°C. Purified transcripts were heat-renatured with the protocol described above and analysed on a DNAPAC-PA100 analytical column (4 × 250 mm, 13.5 μm, Thermo Fisher Scientific) with the same gradients, at a flow rate of 1 ml/min.

Production of AA-minitRNAs with dFx

MinitRNAs were aminoacylated by dFx with 3,5-dinitrobenzyl esters (DBE) of L-alanine or L-glutamate (Supplementary Figure S2). These chemically activated amino acids were synthesized according to standard procedures (22,32). Standard aminoacylation conditions were used (29): 25 μM minitRNA and 37.5 μM of the corresponding dFx were mixed in 50 mM HEPES-KOH pH 7.5 buffer, heated at 95°C for 2 min, and then allowed to cool at room temperature for 5 min. We added 600 mM $MgCl_2$ and incubated the mixture at room temperature for 5 min and then on ice for 3 min. The reaction was initiated by adding the corresponding DBE-activated amino acid at 5 mM and incubating on ice for 1.75 h for DBE-activated alanine and 3 h for DBE-activated glutamate. Reactions were quenched by adding sodium acetate pH 5.2, subjected to ethanol precipitation and the RNA pellets were stored at −80°C. Pellets were dissolved in 20 mM sodium acetate pH 5.2 and the RNA was renatured by applying a gentle heating/quick cooling protocol: heating to 60°C for 30 s, followed by a rapid decrease in temperature to 5°C. All samples were purified and analysed on DNAPAC-PA100 columns as described above, with the gradients described in Supplementary Table S4.

Enzymatic assays

Dried pellets of the substrates to be tested, AA-tRNAs and AA-minitRNAs, were solubilized in 20 mM sodium acetate pH 5.2 shortly before use and kept on ice during all experiments, to limit deacylation. Enzymatic assays were performed in 100 mM phosphate-sodium buffer pH 7.5, 50 mM KCl, 15 mM $MgCl_2$ and 0.1 mM β-mercaptoethanol. Substrates were added to the solution, which was then incubated for 1 min at 20°C, and reactions were initiated by adding 5 nM *Nbra*-CDPS. Aliquots were withdrawn after different times (see below), acidified with 2% trifluoroacetic acid (TFA) to stop the reaction and mixed with known concentrations of stable isotope-labelled internal standards, for quantification of the cAE and cAA produced in LC-MS/MS analyses, as previously described (16) (see section I.C. of Supplementary Data). The stable isotope-labelled standards, cAE and cAA, each containing one $^{13}C_3$-^{15}N-L-alanine residue, were chemically synthesized (see section I.C.i. of Supplementary Data, Supplementary Schemes S1 and 2, Figures S3 and 4). LC-MS analyses were performed on an Elute SP HPLC chain (Bruker Daltonik GmbH) equipped with a DAD detector coupled via a split system to an Amazon SL ion trap mass spectrometer (Bruker Daltonik GmbH) set in positive mode. Samples were injected onto a Hypercarb column (2 × 150 mm, 3 μm, 100 Å, ACE), at a flow rate of 0.2 ml/min, with a linear gradient from 2 to 42% solvent B at 0.2 ml/min over 20 min (solvent A: 0.1% (v/v) formic acid in H_2O; solvent B: 0.1% (v/v) formic acid in acetonitrile/H_2O (90/10)). Cyclodipeptide concentrations were calculated from the ratio of the EIC peak areas of the analyte and the standard compounds (section I.C.ii. of Supplementary Data and Supplementary Figure S5). For the determination of initial velocities, we collected three aliquots during the first 2 min of incubation and plotted the concentrations obtained at the three different sampling times (Supplementary Figure S10). For endpoint assays, the cyclodipeptides were quantified after incubation for 30 min with the appropriate substrates.

RESULTS

Selection of the model CDPS and its substrates

Choice of the CDPS. The study requires to discriminate the binding of the two substrates. Therefore, it should be carried out on a CDPS that uses two different substrates to produce an heterocyclodipeptide. This is not the case for the two CDPSs that have already been submitted to enzymological studies: Rv2275 uses Tyr-tRNA^{Tyr} as its unique substrate to synthesize cyclo(L-Tyr-L-Tyr) (cYY) (13) and AlbC uses Phe-tRNA^{Phe} more efficiently than any of the Leu-tRNA^{Leu} isoacceptors as the second substrate to mostly produces cFF (16). An attractive candidate for overcoming this issue is the recently identified CDPS from *Nocardia brasiliensis*, *Nbra*-CDPS. Upon its heterologous expression in *E. coli, Nbra*-CDPS uses Ala-tRNA^{Ala} and Glu-tRNA^{Glu}

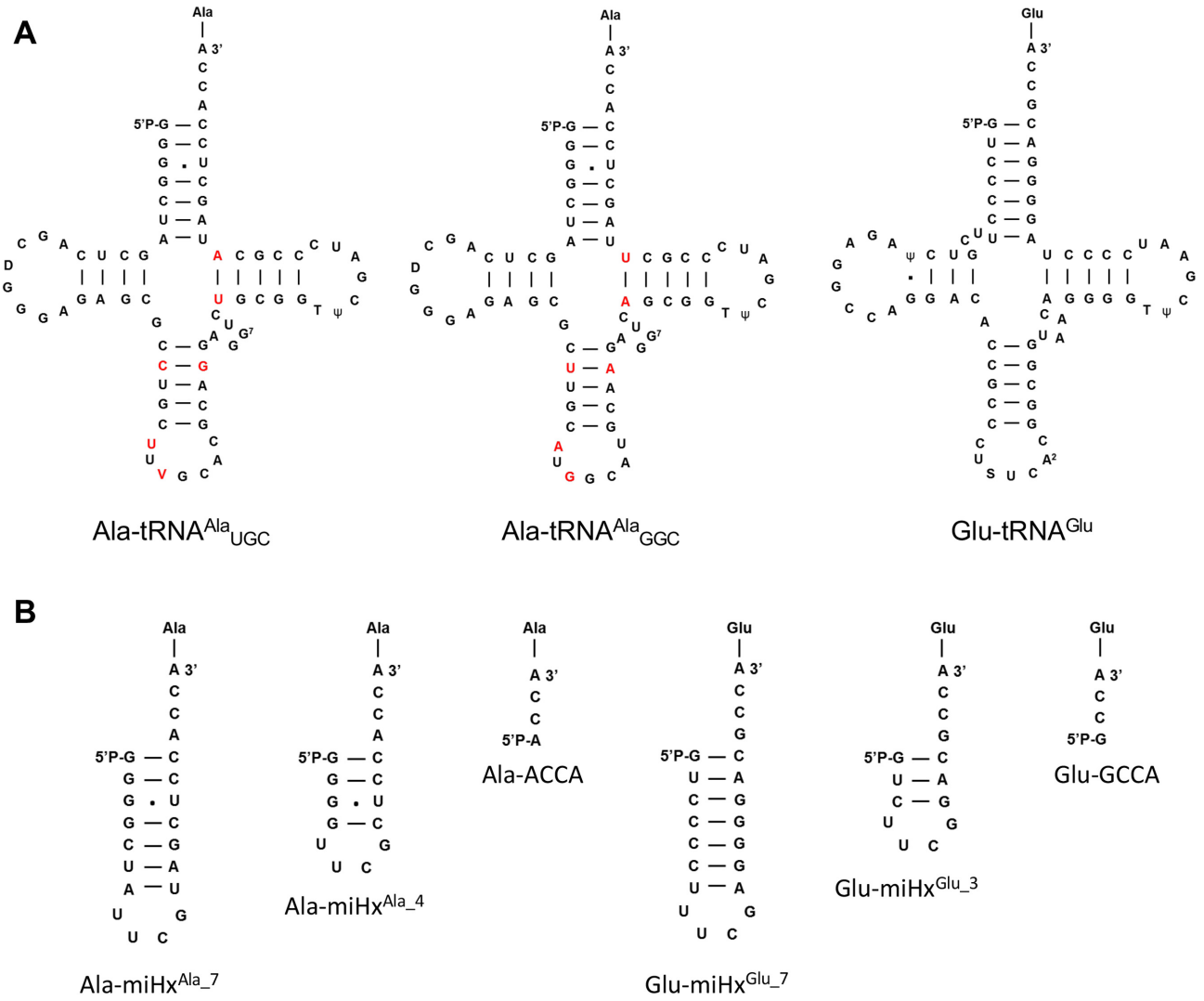

Figure 1. Sequences of substrates and substrates analogues used in the study. (**A**) Secondary structures of *Escherichia coli* aminoacylated tRNAs^{Ala} and tRNA^{Glu}. The differences between the two tRNA^{Ala} isoacceptors are shown in red. (**B**) Secondary structures of the minitRNAs used. Post-transcriptional modifications in full-size RNAs were taken from the MODOMICS database (52) and are abbreviated as follows: D: dihydrouridine; G^7: 7-methylguanosine; V: uridine 5-oxyacetic acid; T: 5-methyluridine; ψ: pseudouridine; S: 5-methylaminomethyl-2-thiouridine; A^2: 2-methyladenosine.

as substrates to produce mostly cAE, only about 2% cAA and no cEE (5). Protein sequence analyses have established that the aminoacyl moiety of Ala-tRNA^{Ala} is accommodated in P1, whereas that of Glu-tRNA^{Glu} is accommodated in the second pocket P2 (5,6). Ala-tRNA^{Ala} can also be accommodated in P2 but it is a very poor substrate, as demonstrated by the very small amounts of cAA produced. *Nbra*-CDPS therefore appears to be an appropriate candidate for use in studies attempting to elucidate the use of the two substrates.

Choice of the substrates. Since *Nbra*-CDPS is active in *E. coli*, we based our study on the use of *E. coli* tRNAs as substrates, as previously described for other characterized CDPSs (4,13,16). The *E. coli* genome encodes one tRNA^{Glu} and two tRNA^{Ala} isoacceptors, tRNA$^{Ala}_{UGC}$ and tRNA$^{Ala}_{GGC}$. Only six nucleotide differences, none of them in the acceptor arms, are found between the two alanine isoacceptors (Figure 1A). All three full-size tRNAs were obtained by overexpression in *E. coli*.

In order to investigate the regions of tRNA^{Ala} and tRNA^{Glu} required for *Nbra*-CDPS activity, we designed a set of minitRNAs based on the sequences of *E. coli* tRNAs (Figure 1B). This set of minitRNAs includes tRNA miHxs, stem-loop RNAs in which the stems corresponded to the acceptor arms of the tRNAs closed by the tetramer loop 5′-UUCG-3′, which is known to favour the stability of short stems (33,34). The two tRNA^{Ala} isoacceptors of *E. coli* have similar acceptor arms and were, therefore, mimicked by the same miHx^{Ala}. We included miHxs with 7 bp stems that mimicked the entire acceptor arm, and the miHxs with the shortest stems predicted to be stable, miHx^{Glu_3} and miHx^{Ala_4} (miHx^{Ala_3} was excluded from the study because the corresponding hairpin conformation was not predicted to be stable) (Supplementary Table S5). Finally, we also included RNA tetramers mimicking the 3′ NCCA tail of the

tRNAs. All minitRNAs were obtained by *in vitro* transcription or chemical synthesis (Supplementary Table S1).

Production of purified flexizyme-aminoacylated minitRNAs

The full procedure for producing AA-minitRNAs was developed with Ala-miHx^{Ala_7}. MiHx^{Ala_7} was synthesized by *in vitro* transcription, purified by anion-exchange chromatography on a semi-preparative DNAPAC column, desalted and lyophilized (see 'Materials and Methods' section). Anion-exchange chromatography was performed under non-denaturing conditions, and miHx^{Ala_7}, like many small RNA hairpins, can fold into different intra- and intermolecular conformations (Supplementary Table S5). We ensured that the most stable intramolecular conformation was favoured by heating and rapidly cooling miHx^{Ala_7} samples to ensure their renaturation before purification and analysis (35). Such renaturation protocol had a dramatic effect on HPLC profiles. For example, renaturation decreased the number of peaks observed after the injection of purified miHx^{Ala_7} from two to one (Supplementary Figure S13). We alanylated miHx^{Ala_7} with dFx under standard conditions. A rate of about 60% alanylation was achieved, as demonstrated by acid-PAGE (polyacrylamide gel electrophoresis) analysis (Supplementary Figure S14A). We developed a new procedure for purifying Ala-miHx^{Ala_7} and separating it from residual miHx^{Ala_7}, based on the use of the DNAPAC column. We assumed that the change in charge following RNA aminoacylation (the primary α-amine function of amino acids is positively charged in neutral or slightly acidic conditions) would induce a different pattern of behaviour during anion exchange chromatography. A comparison of the chromatogram obtained for the alanylation miHx^{Ala_7} with that obtained for purified miHx^{Ala_7} revealed a new peak, with a shorter retention time (Supplementary Figure S14B). The corresponding eluted compound was purified and its characterization by acid-PAGE analysis and MALDI-TOF-MS showed it to be Ala-miHx^{Ala_7} (Supplementary Figure S14A and C). Figure 2 sums up the various steps in the purification process, from the crude *in vitro* transcription reaction products to purified Ala-miHx^{Ala_7}. Ala-miHx^{Ala_7} deacylation occurred during purification, but often at rates of less than 20%, as shown by the ratio of the areas of the peaks corresponding to Ala-miHx^{Ala_7} and miHx^{Ala_7} in purified Ala-miHx^{Ala_7} (Figure 2D). The aminoacylation reaction and the purification process could easily be scaled up for the production of several tens of micrograms of Ala-miHx^{Ala_7}. Interestingly, the purification protocol also effectively separated and purified the dFx from the reaction mixture (Supplementary Figure S14B). It was therefore possible to purify the dFx and to reuse them several times, with no loss of efficiency.

We performed a similar experiment for the production of Glu-miHx^{Glu_7}. Chemically synthesized miHx^{Glu_7} was renatured and then glutamylated with dFx. Aminoacylation was analysed on the DNAPAC column. The chromatogram obtained was similar to that for Ala-miHx^{Ala_7}, with the presence of an additional peak relative to the chromatogram of miHx^{Glu_7}, with a shorter retention time than the peak corresponding to miHx^{Glu_7} (Supplementary Figure S15A). MALDI-TOF confirmed that the eluted compound was

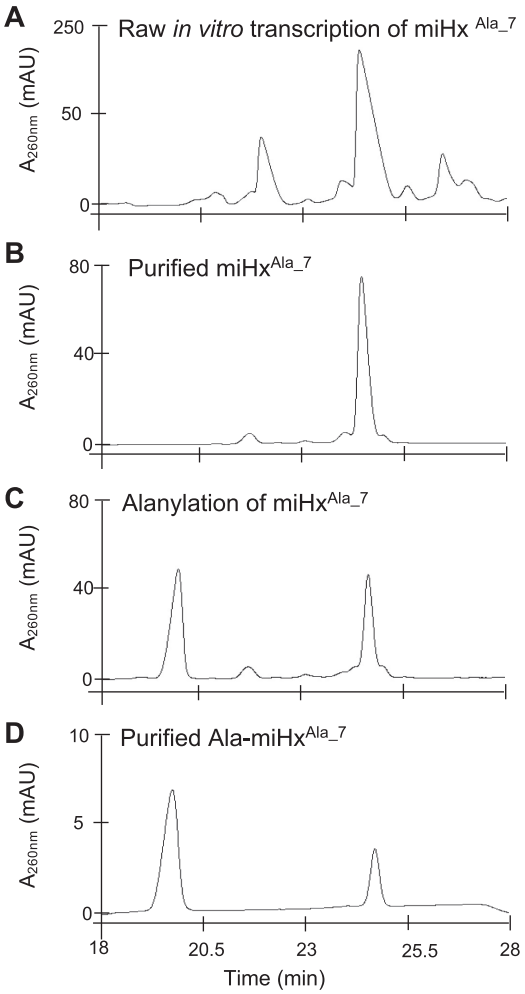

Figure 2. Purification of Ala-miHx^{Ala_7}. Chromatograms corresponding to the injection onto the DNAPAC column of (**A**) 20 μg crude *in vitro* transcription mixture for miHx^{Ala_7}, (**B**) 1 μg purified miHx^{Ala_7}, (**C**) the alanylation of 1 μg miHx^{Ala_7} with a dFx and (**D**) 0.25 μg purified Ala-miHx^{Ala_7}.

Glu-miHx^{Glu_7} (Supplementary Figure S15B). Despite the separation being performed with similar gradients, the glutamylation of miHx^{Glu_7} resulted in a lower shift in retention time (about 2.8 min) than the alanylation of miHx^{Ala_7} (about 5 min). This may be due to the negative charge on the side chain of glutamate at pH 5.5, partly compensating for the effect of the additional positive charge on the backbone amine group.

Similar experiments were performed with smaller minitRNAs, which were also retained on the DNAPAC column. The length of the minitRNA conditioned its retention time, with shorter minitRNAs having shorter retention times (Supplementary Figure S16). Anion-exchange chromatography was used to analyse the flexizyme aminoacylation reactions for minitRNAs. Additional peaks corresponding to AA-minitRNAs were observed. Aminoacylation yields were found to be about 60% for minitRNAs^{Ala} and 45% for minitRNAs^{Glu}, consistent with the results of Prof. Suga and coworkers (22,23). By scaling up the reactions, we were able to obtain several nmoles of aminoacy-

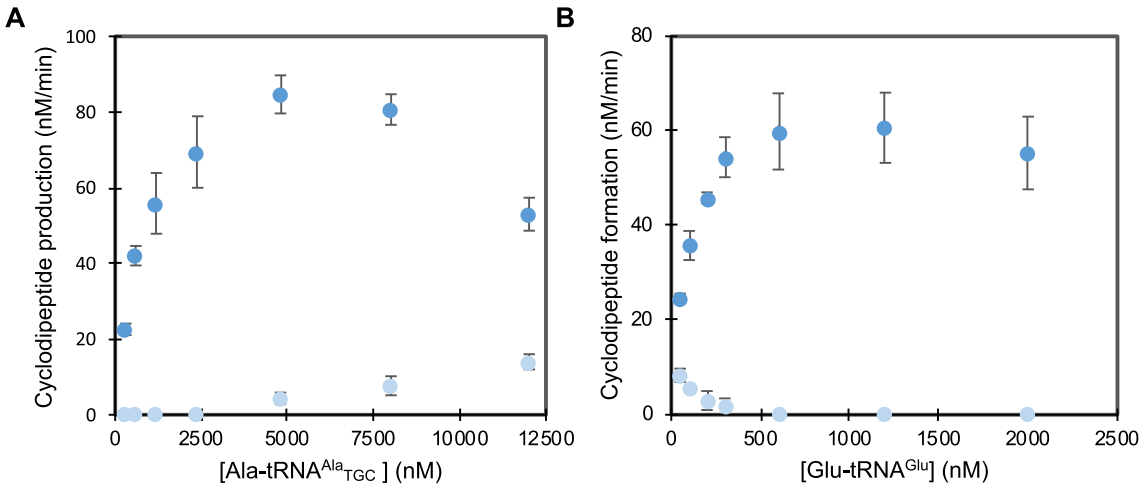

Figure 3. Kinetic studies of the interaction of *Nbra*-CDPS with its AA-tRNA substrates. Initial rates of cAE (dark blue) and cAA (light blue) production were measured with (**A**) 600 nM Glu-tRNA^{Glu} and various concentrations of Ala-tRNA$^{Ala}_{UGC}$ and (**B**) 1200 nM Ala-tRNA$^{Ala}_{UGC}$ and various concentrations of Glu-tRNA^{Glu}. Error bars indicate the standard error between triplicates. The cyclodipeptide titration curves used to determine initial rates are shown in Supplementary Figure S10.

lated minitRNAs. The identity of the aminoacylated products was confirmed by MALDI-TOF (Supplementary Figure S17). Deacylation during the purification process did not exceed 20% for alanylated minitRNAs and 10% for glutamylated minitRNAs, as shown by analytical anion-exchange chromatography.

The anion-exchange chromatography method presented here was also used for time-course analyses of aminoacylation by dFx and to determine optimal reaction times. These optimal reaction times were found to be 1.75 h for minitRNA^{Ala} and 3 h for minitRNA^{Glu}(Supplementary Figure S18), which is coherent with previously reported data.

Principle and optimization of the enzymatic assay

Previous enzymological studies of CDPSs used coupled CDPS/AARS assays, in which *E. coli* AA-tRNAs are generated *in situ* by *E. coli* AARSs (10,16). This approach is unsuitable for studies of minitRNAs, most of which are not AARS substrates. We therefore developed a direct assay, in which tRNAs and their minitRNA analogues were aminoacylated and purified before their testing as substrates for cyclodipeptide production by *NBra*-CDPS. Standard procedures were used for the AARS-based aminoacylation of full-size tRNAs and their purification. For minitRNAs, the new method of production described above was used.

Careful optimization of the various components and parameters of the assay was required to maximize the cyclodipeptide-synthesizing activity of *Nbra*-CDPS and to ensure that the spontaneous hydrolysis of the aminoacyl-linkage of the substrates to tRNAs during the assays could be neglected. Preliminary results suggested that the activity of *Nbra*-CDPS was similar for the two tRNA^{Ala} isoacceptors. We therefore optimized the *in vitro* assay with Ala-tRNA$^{Ala}_{UGC}$ before performing accurate comparison between both isoacceptors. The nature of buffer greatly affected *Nbra*-CDPS activity. The two buffers previously used in enzymatic assays, Tris–HCl and HEPES-KOH (10,16), strongly inhibit *Nbra*-CDPS activity (Supplementary Figure S6). The observed inhibition may be due to the binding of HEPES in the P1 pocket of *Nbra*-CDPS, as previously observed for CHES and CAPSO in the crystal structure of the CDPS YvmC (14). Sodium phosphate was selected as a more appropriate buffer in this context. *Nbra*-CDPS activity significantly increased as pH increased from 7.00 to 7.75 (Supplementary Figure S7A). However,the spontaneous deacylation of the substrates is also favoured by increasing pH (36). We limited this reaction by performing the assay at pH 7.50. AA-tRNA deacylation is also favoured by increasing temperature (37), and the activity of *Nbra*-CDPS is similar at 20°C and 30°C (Supplementary Figure S7B). We therefore performed reactions at 20°C. Finally, 5 nM *Nbra*-CDPS was shown to be a convenient concentration for the measurement of initial reaction rates (Supplementary Figure S8). In these conditions, the maximal duration of the assay required for the determination of initial reaction rates was 2 min. In order to confirm that the deacylation occurring over such time ranges is negligible, we used the chromatographic method described above to study the spontaneous deacylation of Ala-miHx^{Ala_7} and Glu-miHx^{Glu_7} in the conditions of the cyclodipeptide production assay. We found the half-life of these products to be 60 and 145 min, respectively (Supplementary Figure S19 and Table S6), consistent with previous reports showing alanylated-tRNAs to be the least stable AA-tRNAs (32). Based on these findings, we estimated that spontaneous deacylation rates were limited to 2.3% for alanylated substrates and 1.0% for glutamylated substrates after 2 min (maximal duration of the assays used to calculate initial reaction rates) (Supplementary Table S6).

Enzymatic characterization of *Nbra*-CDPS using its two AA-tRNA substrates

We began by characterizing the behaviour of the first substrate of *Nbra*-CDPS, Ala-tRNA^{Ala}, by measuring the ini-

tial rate of reaction for a fixed concentration of Glu-tRNA^{Glu} and a variable concentration of Ala-tRNA^{Ala}. We obtained similar results for the two isoacceptors (Supplementary Figure S9), suggesting that the six nucleotides in the TψC stem and the anticodon stem-loop that differ between these isoacceptors (Figure 1A) are not involved in substrate recognition. We therefore performed all subsequent experiments with Ala-tRNA$^{Ala}_{UGC}$. We measured cyclodipeptide production with 600 nM Glu-tRNA^{Glu} and various concentrations of Ala-tRNA$^{Ala}_{UGC}$, ranging from 300 nM to 12 μM (Figure 3A and Supplementary Figure S10). For concentrations of Ala-tRNA$^{Ala}_{UGC}$ up to about 4.8 μM, the initial rate of cAE production increased with increasing substrate concentrations, and almost no cAA production was detected. At higher Ala-tRNA$^{Ala}_{UGC}$ concentrations, saturable rates of cAE production appeared to be achieved, followed by a decrease in rate with increasing substrate concentrations. The rate of concomitant cAA production was low, and increased with increasing substrate concentration.

Similar experiments were performed to characterize the second substrate, with Ala-tRNA$^{Ala}_{UGC}$ at a constant concentration of 600 nM and various concentrations of Glu-tRNA^{Glu}. However, saturable rates of cAE production were observed regardless of the concentration of Glu-tRNA^{Glu} used. We therefore tested lower concentrations of Glu-tRNA^{Glu} with a higher fixed concentration of Ala-tRNA$^{Ala}_{UGC}$ (1200 nM) to increase cyclodipeptide production and facilitate detection (Figure 3B and Supplementary Figure S10). Up until a concentration of about 600 nM Glu-tRNA^{Glu}, the initial rate of cAE production increased and the rate of cAA production decreased. At higher Glu-tRNA^{Glu} concentrations, saturable rates were observed, followed by a decrease in the rate of production for cAE and cAA production was not detected.

Taken together, the results clearly demonstrate that competition and/or inhibition occur at the two binding sites. When Ala-tRNA^{Ala} is present in large excess, it replaces Glu-tRNA^{Glu} as the second substrate. However, cAA production requires a large molar excess of Ala-tRNA^{Ala} relative to Glu-tRNA^{Glu} (at least 4-fold) and cAA levels remain much lower than cAE levels (Figure 3), confirming the strong preference of the enzyme for Glu-tRNA^{Glu} as the second substrate. When Glu-tRNA^{Glu} is present in large excess, a decrease in cAE production is observed, suggesting that Glu-tRNA^{Glu} may act as an inhibitor at the first or another binding site (Figure 3B). These results reflect the complexity of the reaction catalysed by *Nbra*-CDPS, making it difficult to determine kinetic parameters accurately. However, the results seem to indicate a large difference in the affinity of *Nbra*-CDPS for its two substrates, with maximal initial rates reached at a concentration of about 5000 nM for Ala-tRNA$^{Ala}_{UGC}$ and about 600 nM for Glu-tRNA^{Glu}. In both cases, the 'pre-saturation' increase in initial rates could be modelled with a Michaelis–Menten equation, yielding apparent K_M values of 930 ± 114 nM for Ala-tRNA$^{Ala}_{UGC}$ and 93 ± 8 nM for Glu-tRNA^{Glu} (Supplementary Figure S11). This suggests that the affinity of the second binding site for Glu-tRNA^{Glu} is greater than that of the first binding site for Ala-tRNA$^{Ala}_{UGC}$. Apparent k_{cat} values for *Nbra*-CDPS were estimated at 0.33 s^{-1} for Ala-tRNA$^{Ala}_{UGC}$ and 0.25 s^{-1} for Glu-tRNA^{Glu} (Supplementary Figure S11), although it is clear that there is a risk of these values being substantially underestimated due to the observed competition and/or inhibition. Apparent catalytic efficiencies were estimated by calculating k_{cat}^{app}/K_M^{app} ratios. We obtained values of 0.4×10^6 $M^{-1}.s^{-1}$ for Ala-tRNA^{Ala} as the first substrate and 2.7×10^6 $M^{-1}.s^{-1}$ for Glu-tRNA^{Glu} as the second substrate.

This study using entire AA-tRNAs confirmed that *Nbra*-CDPS was a relevant model for discriminative studies of the use of two substrates and set reference values for the comparative study of shortened substrates.

Enzymatic characterization of *Nbra*-CDPS using AA-mini-tRNAs as substrates

We first investigated the use, by *Nbra*-CDPS, of Ala-miHx^{Ala_7} and Glu-miHx^{Glu_7}, which mimic the entire acceptor stems of tRNA^{Ala} and tRNA^{Glu}, with an approach similar to that used for AA-tRNA substrates (i.e. by measuring the initial rate of cyclodipeptide production for a range of concentrations of Ala-miHx^{Ala_7} in the presence of 600 nM Glu-tRNA^{Glu} or for a range of concentrations of Glu-miHx^{Glu_7} in the presence of 1200 nM Ala-tRNA$^{Ala}_{UGC}$). The results were compared with those obtained with the corresponding AA-tRNAs (Figure 4A and B). The initial rates of cAE production obtained with Ala-miHx^{Ala_7} were very similar to those obtained with Ala-tRNA$^{Ala}_{UGC}$ (Figure 4A), indicating that Ala-miHx^{Ala_7} was as good a substrate as Ala-tRNA^{Ala} at the first binding site. As for Ala-tRNA$^{Ala}_{UGC}$, no cAA was produced at the concentrations tested (Supplementary Figure S12). With Glu-miHx^{Glu_7}, the initial rates of reaction was also close to that for Glu-tRNA^{Glu}. When using low and increasing concentrations of Glu-miHx^{Glu_7}, the increase in cAE production (Figure 4B) and the decrease in cAA production (Supplementary Figure S12) was slightly faster than with Glu-tRNA^{Glu}. When used at high concentrations, Glu-miHx^{Glu_7} inhibited cAE production even more strongly than Glu-tRNA^{Glu}. This suggests that Glu-miHx^{Glu_7} is at least as good a substrate as Glu-tRNA^{Glu} and that it competes more efficiently than Glu-tRNA^{Glu} with Ala-tRNA^{Ala} for the second binding site.

We then performed similar experiments using aminoacylated tetramer oligonucleotides mimicking the 3′ NCCA of tRNAs (Figure 1B). No cAE production was detected with Ala-ACCA and Glu-tRNA^{Glu} or Glu-GCCA and Ala-tRNA$^{Ala}_{UGC}$ (Figure 4A and B). The 3′ tails of the tRNAs are, therefore, clearly not sufficient for use as substrates by *Nbra*-CDPS in the conditions of our assay. Moreover, as the low amount of cAA remains constant when Ala-tRNA^{Ala} is used with increasing concentrations of Glu-GCCA (Figure 4B and Supplementary Figure S12B), this analogue is not an efficient competitor for the second binding site of the enzyme.

The *in vitro* assay do not appear to be suitable for the characterization of very poor substrates, because of the detection threshold for cyclodipeptide production (section I.C.ii of Supplementary Data). We therefore used an endpoint assay, in which cyclodipeptide production was quantified after incubation for 30 min with the substrates (it

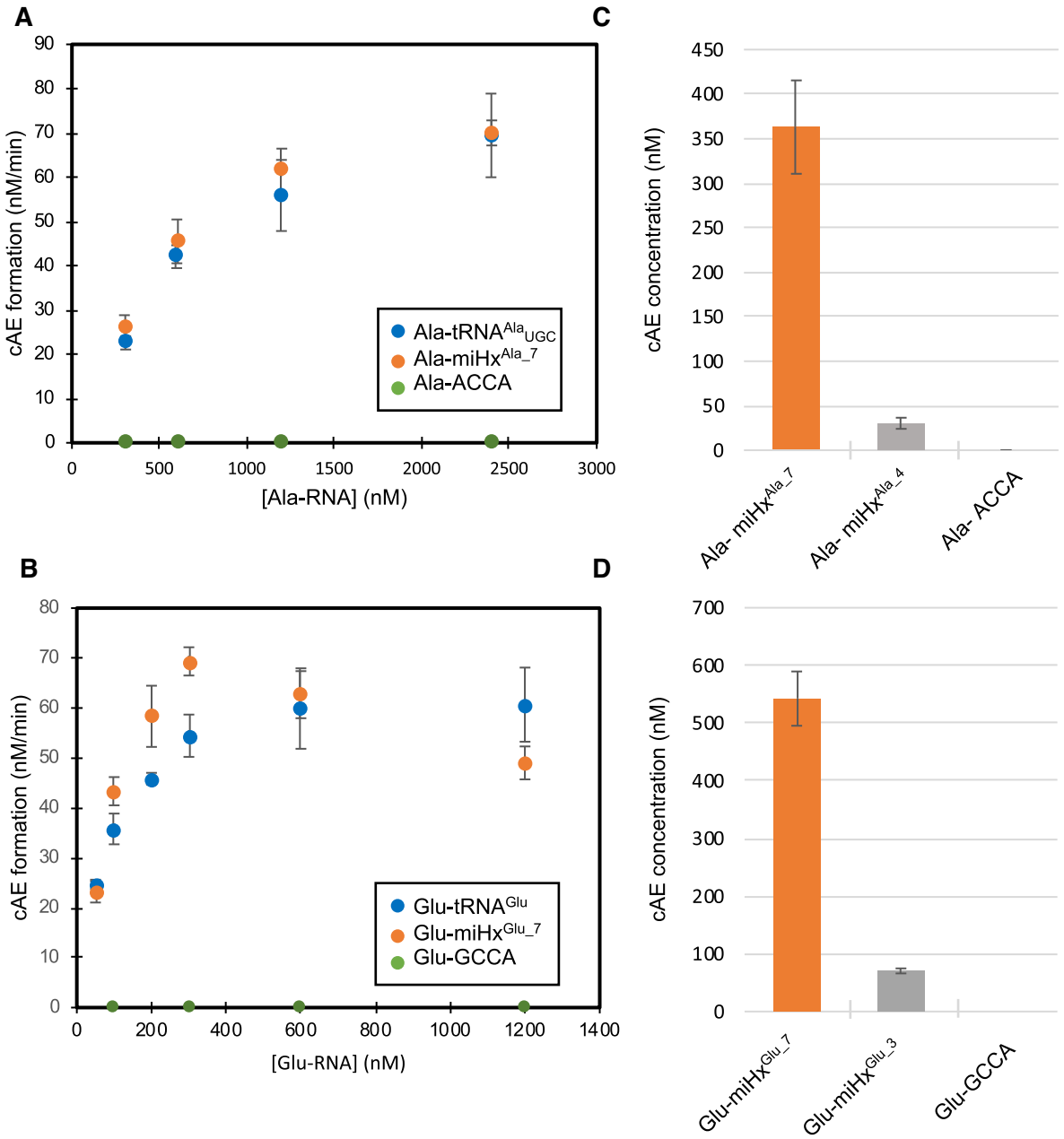

Figure 4. Kinetic study of the interaction of *Nbra*-CDPS with AA-minitRNA substrates. Initial rates of cAE production were measured with (**A**) 600 nM Glu-tRNA^{Glu} and various concentrations of Ala-minitRNA^{Ala} and (**B**) 1200 nM Ala-tRNA$^{Ala}_{UGC}$ and various concentrations of Glu-minitRNA^{Glu}. End-point assays were performed with (**C**) 600 nM Glu-tRNA^{Glu} and 600 nM Ala-minitRNA^{Ala} and (**D**) 1200 nM Ala-tRNA$^{Ala}_{UGC}$ and 600 nM Glu-minitRNA^{Glu}. Error bars indicate the standard errors between duplicates. For the sake of clarity, cAA production is not indicated on Figure 4. Data for cAA production are presented in Supplementary Figure S12.

should be noted that after 30 min incubation in the conditions of the assays deacylation of the substrate could reach up to 29.3 and 13.3%, for alanylated and glutamylated substrates, respectively (Supplementary Table S6)). Upon incubation of 600 nM Ala-ACCA with 600 nM Glu-tRNA^{Glu} or of 600 nM Glu-GCCA with 1200 nM Ala-tRNA$^{Ala}_{UGC}$, no cAE production was detected, confirming that these aminoacylated 4-mer cannot act efficiently as substrates of *Nbra*-CDPS (Figure 4C and D). Upon incubation of Glu-GCCA, cAA production was detected (Supplementary Figure S12D), as might be expected for an inefficient competitor of Ala-tRNA^{Ala} at the second biding site.

Finally, we used the same endpoint assay to evaluate the activity of *Nbra-CDPS* with the miHxs with the shortest stable stems. We found that Ala-miHx^{Ala_4} could act as a substrate for *Nbra*-CDPS, but that it was a much poorer substrate than Ala-miHx^{Ala_7} (Figure 4C). Similarly, Glu-miHx^{Glu_3} was found to act as a substrate of *Nbra*-CDPS, but much less cAE was produced than with Glu-miHx^{Glu_7} (Figure 4D).

DISCUSSION

We show here that *Nbra*-CDPS is a relevant model for studies aiming to discriminate between the substrates used at the two binding sites of CDPSs. It was not possible to determine kinetic parameters accurately, due to the apparent cross-inhibition or cross-competition of substrates and probable changes in the conformation of the CDPS between its free, aminoacyl and dipeptidyl states. However, our data suggest that *Nbra*-CDPS has significantly different affinities for its two substrates: the affinity of the first binding site for Ala-tRNA^{Ala} appears to be lower than that of the second binding site for Glu-tRNA^{Glu}. Only two kinetic studies on CDPSs have been published, both focused on the use of Tyr-tRNA^{Tyr} by the cYY-producing CDPS Rv2275 (13,38). However, the authors of both studies used a one-substrate model to estimate these kinetic parameters, which is incompatible with a ping-pong mechanism involving two substrates at two different binding sites, making it impossible to discriminate between these two sites for the purposes of characterization.

The feasibility of direct *in vitro* CDPS assays combined with AA-minitRNA production by flexizymes made it possible to investigate the use of various substrates modified in the RNA part at each of the two binding sites. We used this approach to improve our understanding of the regions of the two tRNAs required for CDPS activity. We were primarily interested in determining the role of the acceptor arms of tRNAs, as we previously demonstrated the involvement of this region in the interaction with CDPSs (16,17). We demonstrated that AA-miHxs, which mimic the entire 7 bp stem of tRNA^{Ala} and tRNA^{Glu} acceptor arms, are at least as good as the corresponding AA-tRNAs in terms of their ability to act as substrates for *Nbra*-CDPS. By contrast, no activity was observed when the substrates tested were limited to the aminoacylated 3′ tails. The tRNA acceptor arms are, therefore, required at the two binding sites for *Nbra*-CDPS activity, whereas the three stem-loops of tRNAs are fully dispensable. We explored the minimal substrates of CDPSs further, by focusing on the smallest stable microhelices, Ala-miHx^{Ala_4} and Glu-miHx^{Glu_3}. We found that these microhelices were poorer substrates than the corresponding entire AA-miHxs, suggesting that *Nbra*-CDPS may require distal nucleotides from both acceptor arms. However, one major concern with these shorter miHxs is that the tetramer loops introduced to close the miHxs may hamper the interaction with the binding sites of the enzymes by causing artificial steric hindrance. The promising results obtained in this study suggest that flexizyme technology will pave the way for further biochemical and structural investigation of CDPS specificity and for elucidating the specificity determinants of CDPS and other enzymes using AA-tRNAs as substrates.

Other families of enzymes have evolved the ability to hijack AA-tRNAs from their canonical role for various types of reaction (1). In particular, three families of enzymes and their mode of interaction with their AA-tRNA substrates have been investigated in detail: class I lanthipeptide dehydratases (LanBs), which use Glu-tRNA^{Glu} for the successive glutamylation and dehydrogenation of serine and threonine residues in ribosomally synthesized and post-translationally modified peptides (39), Fem transferases X (FemX), which transfer the alanyl moiety of Ala-tRNA^{Ala} to the UDP-MurNAc-pentapeptide during peptidoglycan biosynthesis (40), and L/F transferases, which transfer the leucyl moiety of Leu-tRNA^{Leu} (and, to a lesser extent, the phenylalanyl moiety of Phe-tRNA^{Phe}) to the N-terminus of proteins as a label for targeted degradation (41). Interestingly, despite their differences in substrate specificity and function, LanBs, FemX and L/F transferases have all been shown, via various experimental strategies, to interact with the acceptor arm of the tRNA moieties of their substrates.

A first approach to investigating the tRNA regioselectivity of AA-tRNA-utilizing enzymes is based on the use of mutant tRNAs that are acylated by AARSs. Mutations are introduced into the tRNAs, which are then assayed as substrates to assess the effect of the mutations on their activity. An effect of the mutation is interpreted as indicating that the mutated nucleotide is involved in recognition by the enzyme. This approach has been used to show that L/F transferases and FemX interact with up to the first five and four base pairs, respectively, of the acceptor arms of their substrates (42,43). Similar studies have also demonstrated that the LanB-like MibB interacts specifically with the discriminator base A_{73} and the nucleotide U_{72} within the Glu-tRNA^{Glu} (44), and that the CDPS AlbC interacts with the first base pair of its second AA-tRNA substrate (16). However, methods based on the use of AARSs for aminoacylation are intrinsically limited in terms of the range of RNA acceptors that can be tested, because the specificity determinants required for aminoacylation must be conserved (45). One interesting way to get around this limitation is to synthesize AA-tRNA analogues by chemoenzymatic methods, through the enzymatic ligation of aminoacylated dinucleotide to tRNA analogues lacking two nucleotides at their 3′ end (46,47). This strategy makes it possible to aminoacylate a much broader range of tRNA-like molecules than AARS-based methods, including shortened tRNA analogues, such as miHx or tRNAs, with mutations of AARS specificity determinants. This approach was used to generate various analogues of Ala-tRNA^{Ala} for the study of FemX, including shortened analogues, such as Ala-miHx^{Ala}, which was shown to be a good substrate of FemX, and various mutated miHxs, which were used to elucidate the role of the nucleotide sequence in determining specificity (31). It would be particularly interesting to apply this strategy to other AA-tRNA-utilizing enzymes, including CDPSs in particular. However, it necessitates the use of 2′-deoxycytidine as the penultimate nucleotide, and preliminary results with such molecules (kindly prepared by our collaborators M. Fonvielle, M. Ethève-Quelquejeu and M. Arthur) and the CDPS AlbC have suggested that this modification induces a decrease CDPS activity. The flexizyme-based production pipeline described here thus constitutes a valuable alternative. Given the infinite diversity of RNA acceptors that can be aminoacylated with flexizymes and to the ability of these ribozymes to use any amino acid, it should be possible to produce AA-minitRNAs with any sequence desired. This would make it possible to dissect out the sequence-dependent recognition of tRNAs at the two binding sites of *Nbra*-CDPS or of other CDPSs.

Three-dimensional structures have been determined for various members of the three families of AA-tRNA-utilizing enzymes (15,39,48–49). Only CDPSs present a Rossmann-fold domain similar to that of class I AARSs (15). Thus, several different folds have evolved the ability to recognize AA-tRNAs. Structures of enzymes in complex with AA-tRNA analogues have also been reported, but the size and intrinsic flexibility of tRNAs have made it impossible to obtain high-resolution structures with full-size substrates. Minimal substrate analogues have, therefore, been used. We previously reported the structure of AlbC in complex with a dipeptidyl intermediate, shedding light on aminoacyl binding by CDPSs (11). In the case of LanBs and L/F transferases, structures have been reported with synthetic analogues of puromycin, which mimic the 3′-terminal aminoacylated adenosines of AA-tRNAs and in which the labile ester bond between the nucleotide and the amino acid is replaced by a stable amide bond (48,50). Using peptidyl-RNA conjugates produced by a solid-phase synthesis/click chemistry approach, Fonvielle *et al*. reported the structure of FemX in complex with a peptidyl-RNA miHx via two base pairs (43). The flexizyme-based production of various aminoacylated RNAs appears to be of great interest for determining the structure of CDPSs (or other AA-tRNA-utilizing enzymes) in complex with such analogues, particularly since the recent report from Prof. Suga and coworkers indicating that flexizymes are active on RNA molecules with a final adenosine residue bearing the 3′-deoxy-3′-amino modification, making it possible to produce analogues in which the ester bond of the aminoacyl linkage is replaced by the more stable amide bond (51).

The diverse methods for obtaining AA-tRNA analogues have different advantages and drawbacks. Methods based on AARSs are simple and efficient, but the spectrum of amino acids and RNA acceptors that can be used is restricted by the natural specificity of these enzymes. The chemoenzymatic synthesis of aminoacylated or peptidylated tRNA analogues provides access to a broad range of AA-tRNA analogues bearing diverse modifications. However, this approach requires the use of 2′-deoxycytidine (dC) as the penultimate nucleotide, which may be problematic if the 2′ hydroxyl of the C_{75} nucleotide of AA-tRNA is involved in the interaction with the enzyme. One of the major limitations of such approaches is that multi-step synthesis routes are not easily reproducible in a typical biological laboratory. Flexizymes constitute a convenient tool for aminoacylation, because they provide good aminoacylation yields in a single step in mild conditions with an almost infinite versatility of amino acids and RNA acceptors. The combination of flexizymes with anion-exchange chromatography presented here constitutes a valuable tool for studies of AA-tRNAs and associated mechanisms, as it can be used to generate a very broad range of aminoacylated RNAs. The application of anion-exchange chromatography to the study and manipulation of small aminoacylated RNAs makes it possible to characterize the proportion of an RNA sample that is aminoacylated, in a precise manner, by HPLC. This approach constitutes an interesting addition to the experimental toolbox used for these molecules, and its accuracy appears to exceed that of the conventional method based on acid-PAGE densitometry. We believe that this method will be of great value to the community of scientists studying the growing number of AA-tRNA-utilizing enzymes.

SUPPLEMENTARY DATA

Supplementary Data are available at NAR Online.

ACKNOWLEDGEMENTS

We thank Magali Frugier, Joëlle Rudinger-Thirion and Matthieu Fonvielle for helpful advice concerning RNA handling and Alexandre Couëtoux for experimental assistance.

FUNDING

French National Research Agency [ANR-14-CE09-0021, ANR-19-CE44-0012]; Commissariat à l'Energie Atomique et aux Energies Alternatives Ph.D. scholarships (to N.C., R.V.). Funding for open access charge: French National Research Agency [ANR-19-CE44-0012].
Conflict of interest statement. None declared.

REFERENCES

1. Moutiez,M., Belin,P. and Gondry,M. (2017) Aminoacyl-tRNA-utilizing enzymes in natural product biosynthesis. *Chem. Rev.*, **117**, 5578–5618.
2. Borthwick,A.D. (2012) 2, 5-diketopiperazines: synthesis, reactions, medicinal chemistry, and bioactive natural products. *Chem. Rev.*, **112**, 3641–3716.
3. Wang,X., Li,Y., Zhang,X., Lai,D. and Zhou,L. (2017) Structural diversity and biological activities of the cyclodipeptides from fungi. *Molecules*, **22**, 2026.
4. Gondry,M., Sauguet,L., Belin,P., Thai,R., Amouroux,R., Tellier,C., Tuphile,K., Jacquet,M., Braud,S., Courçon,M. *et al.* (2009) Cyclodipeptide synthases are a family of tRNA-dependent peptide bond-forming enzymes. *Nat. Chem. Biol.*, **5**, 414–420.
5. Jacques,I.B., Moutiez,M., Witwinowski,J., Darbon,E., Martel,C., Seguin,J., Favry,E., Thai,R., Lecoq,A., Dubois,S. *et al.* (2015) Analysis of 51 cyclodipeptide synthases reveals the basis for substrate specificity. *Nat. Chem. Biol.*, **11**, 721–731.
6. Gondry,M., Jacques,I., Thai,R., Babin,M., Canu,N., Seguin,J., Belin,P., Pernodet,J.-L. and Moutiez,M. (2018) A comprehensive overview of the cyclodipeptide synthase family enriched with the characterization of 32 new enzymes. *Front. Microbiol.*, **9**, doi:10.3389/fmicb.2018.00046.
7. Canu,N., Moutiez,M., Belin,P. and Gondry,M. (2020) Cyclodipeptide synthases: a promising biotechnological tool for the synthesis of diverse 2, 5-diketopiperazines. *Nat. Prod. Rep.*, **37**, 312–321.
8. Giessen,T. and Marahiel,M. (2014) The tRNA-dependent biosynthesis of modified cyclic dipeptides. *Int. J. Mol. Sci.*, **15**, 14610–14631.
9. Belin,P., Moutiez,M., Lautru,S., Seguin,J., Pernodet,J.-L. and Gondry,M. (2012) The nonribosomal synthesis of diketopiperazines in tRNA-dependent cyclodipeptide synthase pathways. *Nat. Prod. Rep.*, **29**, 961–979.
10. Sauguet,L., Moutiez,M., Li,Y., Belin,P., Seguin,J., Le Du,M.H., Thai,R., Masson,C., Fonvielle,M., Pernodet,J.L. *et al.* (2011) Cyclodipeptide synthases, a family of class-I aminoacyl-tRNA synthetase-like enzymes involved in non-ribosomal peptide synthesis. *Nucleic Acids Res.*, **39**, 4475–4489.
11. Moutiez,M., Schmitt,E., Seguin,J., Thai,R., Favry,E., Belin,P., Mechulam,Y. and Gondry,M. (2014) Unravelling the mechanism of non-ribosomal peptide synthesis by cyclodipeptide synthases. *Nat. Commun.*, **5**, doi:10.1038/ncomms6141.
12. Schmitt,E., Bourgeois,G., Gondry,M. and Aleksandrov,A. (2018) Cyclization reaction catalyzed by cyclodipeptide synthases relies on a conserved tyrosine residue. *Sci. Rep.*, **8**, 7031.

13. Vetting,M.W., Hegde,S.S. and Blanchard,J.S. (2010) The structure and mechanism of the *Mycobacterium tuberculosis* cyclodityrosine synthetase. *Nat. Chem. Biol.*, **6**, 797–799.
14. Bonnefond,L., Arai,T., Sakaguchi,Y., Suzuki,T., Ishitani,R. and Nureki,O. (2011) Structural basis for nonribosomal peptide synthesis by an aminoacyl-tRNA synthetase paralog. *Proc. Natl. Acad. Sci. U.S.A.*, **108**, 3912–3917.
15. Bourgeois,G., Seguin,J., Babin,M., Belin,P., Moutiez,M., Mechulam,Y., Gondry,M. and Schmitt,E. (2018) Structural basis for partition of the cyclodipeptide synthases into two subfamilies. *J. Struct. Biol.*, **203**, 17–26.
16. Moutiez,M., Fonvielle,M., Belin,P., Favry,E., Arthur,M. and Gondry,M. (2014) Specificity determinants for the two tRNA substrates of the cyclodipeptide synthase AlbC from *Streptomyces noursei*. *Nucleic Acids Res.*, **42**, 7247–7258.
17. Bourgeois,G., Seguin,J., Babin,M., Gondry,M., Mechulam,Y. and Schmitt,E. (2020) Structural basis of the interaction between cyclodipeptide synthases and aminoacylated tRNA substrates. *RNA*, doi:10.1261/rna.075184.120.
18. Kobayashi,T., Nurekil,O., Ishitani,R., Yaremchuk,A., Tukalo,M., Cusack,S., Sakamoto,K. and Yokoyama,S. (2003) Structural basis for orthogonal tRNA specificities of tyrosyl-tRNA synthetases for genetic code expansion. *Nat. Struct. Biol.*, **10**, 425–432.
19. Francklyn,C. and Schimmel,P. (1989) Aminoacylation of RNA minihelices with alanine. *Nature*, **337**, 478–481.
20. Frugier,M., Florentz,C. and Giegé,R. (1994) Efficient aminoacylation of resected RNA helices by class II aspartyl-tRNA synthetase dependent on a single nucleotide. *EMBO J.*, **13**, 2218–2226.
21. Passioura,T. and Suga,H. (2014) Flexizymes, their evolutionnary history and diverse utilities. *Top. Curr. Chem.*, **11**, 331–346.
22. Murakami,H., Ohta,A., Ashigai,H. and Suga,H. (2006) A highly flexible tRNA acylation method for non-natural polypeptide synthesis. *Nat. Methods*, **3**, 357–359.
23. Fujino,T., Kondo,T., Suga,H. and Murakami,H. (2019) Exploring of minimal RNA substrate of flexizymes. *Chembiochem*, **20**, 1959–1965.
24. Ellinger,T. and Ehricht,R. (1998) Single-step purification of T7 RNA polymerase with a 6-histidine tag. *Biotechniques*, **24**, 718–720.
25. Beuning,P.J., Yang,F., Schimmel,P. and Musier-Forsyth,K. (2002) Specific atomic groups and RNA helix geometry in acceptor stem recognition by a tRNA synthetase. *Proc. Natl. Acad. Sci. U.S.A.*, **94**, 10150–10154.
26. Dubois,D.Y., Blais,S.P., Huot,J.L. and Lapointe,J. (2009) AC-truncated glutamyl-tRNA synthetase specific for $tRNA^{Glu}$ is stimulated by its free complementary distal domain: mechanistic and evolutionary implications. *Biochemistry*, **48**, 6012–6021.
27. Belin,P., Le Du,M.H., Fielding,A., Lequin,O., Jacquet,M., Charbonnier,J.-B., Lecoq,A., Thai,R., Courçon,M., Masson,C. *et al.* (2009) Identification and structural basis of the reaction catalyzed by CYP121, an essential cytochrome P450 in *Mycobacterium tuberculosis*. *Proc. Natl. Acad. Sci. U.S.A.*, **106**, 7426–7431.
28. Mechulam,Y., Guillon,L., Yatime,L., Blanquet,S. and Schmitt,E. (2007) Protection-based assays to measure aminoacyl-tRNA binding to translation initiation factors. *Methods Enzymol.*, **430**, 265–281.
29. Goto,Y., Katoh,T. and Suga,H. (2011) Flexizymes for genetic code reprogramming. *Nat. Protoc.*, **6**, 779–790.
30. Konarska,M.M. and Sharp,P.A. (1990) Structure of RNAs replicated by the DNA-dependent T7 RNA polymerase $_{L}$-amino acids. *Cell*, **63**, 609–618.
31. Fonvielle,M., Chemama,M., Villet,R., Lecerf,M., Bouhss,A., Valéry,J.M., Ethève-Quelquejeu,M. and Arthur,M. (2009) Aminoacyl-tRNA recognition by the FemXWv transferase for bacterial cell wall synthesis. *Nucleic Acids Res.*, **37**, 1589–1601.
32. Peacock,J.R., Walvoord,R.R., Chang,A.Y. and Kozlowski,M.C. (2014) Amino acid-dependent stability of the acyl linkage in aminoacyl-tRNA. *RNA*, **20**, 758–764.
33. Tuerk,C., Gauss,P., Thermes,C., Groebe,D.R., Gayle,M., Guild,N., Stormo,G., D'Aubenton-Carafa,Y., Uhlenbeck,O.C. and Tinoco,I. (1988) CUUCGG hairpins: extraordinarily stable RNA secondary structures associated with various biochemical processes. *Proc. Natl. Acad. Sci. U.S.A.*, **85**, 1364–1368.
34. Antao,V.P., Lai,S.Y. and Tinoco,I. (1991) A thermodynamic study of unusually stable RNA and DNA hairpins. *Nucleic Acids Res.*, **19**, 5901–5905.
35. Sun,X., Li,J.M. and Wartell,R.M. (2007) Conversion of stable RNA hairpin to a metastable dimer in frozen solution. *RNA*, **13**, 2277–2286.
36. Schuber,F. and Pinck,M. (1974) On the chemical reactivity of aminoacyl-tRNA ester bond. I - Influence of pH and nature of the acyl group on the rate of hydrolysis. *Biochimie*, **56**, 383–390.
37. Stepanov,V.G. and Nyborg,J. (2002) Thermal stability of aminoacyl-tRNAs in aqueous solutions. *Extremophiles*, **6**, 485–490.
38. Richardson,C.J. and First,E.A. (2015) A continuous tyrosyl-tRNA synthetase assay that regenerates the tRNA substrate. *Anal. Biochem.*, **486**, 86–95.
39. Ortega,M.A., Hao,Y., Zhang,Q., Walker,M.C., van der Donk,W.A. and Nair,S.K. (2014) Structure and mechanism of the tRNA-dependent lantibiotic dehydratase NisB. *Nature*, **517**, 509–512.
40. Maillard,A.P., Biarrotte-Sorin,S., Villet,R., Mesnage,S., Bouhss,A., Sougakoff,W., Mayer,C. and Arthur,M. (2005) Structure-based site-directed mutagenesis of the UDP-MurNAc-pentapeptide-binding cavity of the FemX alanyl transferase from *Weissella viridescens*. *J. Bacteriol.*, **187**, 3833–3838.
41. Leibowitz,M.J. and Soffer,R.L. (1969) A soluble enzyme from *Escherichia coli* which catalyzes the transfer of leucine and phenylalanine from tRNA to acceptor proteins. *Biochem. Biophys. Res. Commun.*, **36**, 47–53.
42. Fung,A.W.S., Leung,C.C.Y. and Fahlman,R.P. (2014) The determination of $tRNA^{Leu}$ recognition nucleotides for *Escherichia coli* L/F transferase. *RNA*, **20**, 1210–1222.
43. Fonvielle,M., Li De La Sierra-Gallay,I., El-Sagheer,A.H., Lecerf,M., Patin,D., Mellal,D., Mayer,C., Blanot,D., Gale,N., Brown,T. *et al.* (2013) The structure of FemXWv in complex with a peptidyl-RNA conjugate: Mechanism of aminoacyl transfer from Ala-$tRNA^{Ala}$ to peptidoglycan precursors. *Angew. Chem. Int. Ed. Engl.*, **52**, 7278–7281.
44. Ortega,M.A., Hao,Y., Walker,M.C., Donadio,S., Sosio,M., Nair,S.K. and Van Der Donk,W.A. (2016) Structure and tRNA specificity of MibB, a lantibiotic dehydratase from actinobacteria involved in NAI-107 biosynthesis. *Cell Chem. Biol.*, **23**, 370–380.
45. Giegé,R., Sissler,M. and Florentz,C. (1998) Universal rules and idiosyncratic features in tRNA identity. *Nucleic Acids Res.*, **26**, 5017–5035.
46. Heckler,T.G., Chang,L.H., Zama,Y., Naka,T., Chorghade,M.S. and Hecht,S.M. (1984) T4 RNA ligase mediated preparation of novel "chemically misacylated" $tRNA^{Phe}$s. *Biochemistry*, **23**, 1468–1473.
47. Robertson,S.A., Ellman,J.A. and Schultz,P.G. (1991) A general and efficient route for chemical aminoacylation of transfer RNAs. *J. Am. Chem. Soc.*, **113**, 2722–2729.
48. Suto,K., Shimizu,Y., Watanabe,K., Ueda,T., Fukai,S., Nureki,O. and Tomita,K. (2006) Crystal structures of leucyl/phenylalanyl-tRNA-protein transferase and its complex with an aminoacyl-tRNA analog. *EMBO J.*, **25**, 5942–5950.
49. Biarrotte-Sorin,S., Maillard,A.P., Delettré,J., Sougakoff,W., Arthur,M. and Mayer,C. (2004) Crystal structures of *Weissella viridescens* FemX and its complex with UDP-MurNAc-Pentapeptide: Insights into FemABX family substrates recognition. *Structure*, **12**, 257–267.
50. Bothwell,I.R., Cogan,D.P., Kim,T., Reinhardt,C.J., van der Donk,W.A. and Nair,S.K. (2019) Characterization of glutamyl-tRNA–dependent dehydratases using nonreactive substrate mimics. *Proc. Natl. Acad. Sci. U.S.A.*, **116**, 17245–17250.
51. Katoh,T. and Suga,H. (2019) Flexizyme-catalyzed synthesis of 3′aminoacyl-NH-tRNAs. *Nucleic Acids Res.*, **47**, e54.
52. Boccaletto,P., MacHnicka,M.A.A., Purta,E., Pitkowski,P., Baginski,B., Wirecki,T.K.K., De Crécy-Lagard,V., Ross,R., Limbach,P.A.A., Kotter,A. *et al.* (2018) MODOMICS: a database of RNA modification pathways. 2017 update. *Nucleic Acids Res.*, **46**, D303–D307.